Biochemical and Biophysical Research Communications 459 (2015) 36–41

Contents lists available at ScienceDirect

Biochemical and Biophysical Research Communications

journal homepage: www.elsevier.com/locate/ybbrc

Computational analysis of the extracellular domain of the Ca^{2+}-sensing receptor: An alternate model for the Ca^{2+} sensing region

Gene A. Morrill*, Adele B. Kostellow, Raj K. Gupta

Department of Physiology and Biophysics, Albert Einstein College of Medicine, Bronx, NY 10461 USA

ARTICLE INFO

Article history:
Received 2 February 2015
Available online 19 February 2015

Keywords:
Ca-sensing receptor
Glutamate receptors
Transmembrane helices
Pore-lining regions
Caveolin
Cholesterol

ABSTRACT

The extracellular Ca^{2+} sensing receptor (CaSR) belongs to Class C G-protein-coupled receptors (GPCRs) which include receptors for amino acids, γ-aminobutyric acid and glutamate neurotransmitters. CaSR has been described as having an extended sequence containing a Ca^{2+} binding pocket within an extracellular amino (N)-terminal domain, called a Venus Fly Trap (VFT) module. CaSR is thought to consist of three domains: 1) a Ca^{2+-}sensory domain, 2) a region containing 7 transmembrane (TM) helices, and 3) a carboxy (C)-terminal tail. We find that SPOCTOPUS (a combination of hidden Markov models and artificial neural networks) predicts that *Homo sapiens* CaSR contains two additional TM helices ($^{190}D-G^{210}$; $^{262}S-E^{282}$), with the second TM helix containing a pore-lining region ($^{265}K-I^{280}$). This predicts that the putative Ca^{2+} sensory domain is within an extracellular loop, N-terminal to the highly conserved heptahelical bundle. This loop contains both the cysteine-rich domain ($^{537}V-C^{598}$) and a 14 residue "linker" sequence ($^{599}I-F^{612}$) thought to support signal transmission to the heptahelical bundle. Thus domain 1 may contain a 189 residue N-terminal extracellular region followed successively by TM-1, a short intracellular loop, TM-2 and a 329 residue extracellular loop; rather than the proposed 620 residue VFT module based on crystallography of the N-terminal region of mGluR1. Since the topologies of the two proteins differ, the published CaSR VFT model is questionable. CaSR also contains multiple caveolin-binding motifs and cholesterol-binding (CRAC/CARC) domains, facilitating localization to plasma membrane lipid rafts. Ion sensing may involve combination of pore-lining regions from CaSR dimers and CaSR-bound caveolins to form ion channels capable of monitoring ionized Ca^{2+} levels.

1. Introduction

The calcium sensing receptor (CaSR) belongs to family C (or III) of G protein-coupled receptors (reviewed in Refs. [1–5]). The human CaSR contains 1078 amino acids: the extracellular Ca^{2+}-sensing domain reportedly consists of 612 N-terminal amino acids and is followed by a 250 amino acid domain containing a highly conserved 7 transmembrane (TM) helix bundle and in turn by a carboxy (C)-terminal tail of about 200 amino acids (reviewed in Ref. [6]). Molecular modeling based on crystallographic structures of a related metabotropic glutamate receptor (mGluR1) [7] suggests that the CaSR extracellular domain resembles a Venus flytrap (VFT)-like motif, a bi-lobed structure with a crevice between the two lobes thought to contain a key binding site for Ca^{2+} [3,8]. The bi-lobed structure containing the Ca^{2+} binding site is tethered to the heptahelical signaling domain (reviewed in Ref. [9]). The VFT is thought to be open in the absence of agonist and to close upon Ca^{2+} binding, thereby causing conformational changes in TM and intracellular domains that initiate signal transduction.

Because the insertion of TM helices into the plasma membrane initiates complex molecular interactions among proteins, lipids and water, the membrane topology of the N-terminal region of CaSR may differ from that predicted by crystallographic analysis of the purified mGluR1. In this study, CaSR and mGluR1 are compared in terms of membrane topology, pore-lining regions, cholesterol binding domains and caveolin binding motifs [10,11]. Comparison of the plasma membrane topology of CaSR and mGluR1 should provide insights into the Ca^{2+} signaling mechanism(s) and indicate whether the Ca^{2+}-sensing region is associated with an N-terminal extracellular Venus Fly Trap (VTF)-like motif.

* Corresponding author.
E-mail addresses: gene.morrill@einstein.yu.edu (G.A. Morrill), kostellow@aol.com (A.B. Kostellow), raj.gupta@einstein.yu.edu (R.K. Gupta).

http://dx.doi.org/10.1016/j.bbrc.2015.02.049

2. Materials and methods

2.1. Materials

The amino acid sequences of *Homo sapiens* extracellular calcium sensing receptor (Accession #P41180) and metabotropic glutamate receptor 1 (Accession #Q13255) were downloaded from the ExPASy Proteonomic Server of the Swiss Institute of Bioinfomatics (http://www.expasy.org; http://www.uniprot.org). About 98% of the protein sequences provided by UniProtKB are derived from the translation of the coding sequences (CDS) which have been submitted to the public nucleic acid databases, the EMBL-Bank/Genbank/DDBJ databases (INSDC). Amino acid sequences were compared using the Pairwise Sequence Alignment software (LALIGN) at http://www.ebi.ac.uk/Tools/services/web lalign/to find internal duplications by calculating non-intersecting local alignments [12]. The Emboss Water protocol (version 36.3.5e Nov, 2012; preload8) used here employs the Smith–Waterman algorithm (with modified enhancements) to calculate the local alignment of two sequences.

2.2. Transmembrane (TM) helix and pore-lining region predictions

To identify possible transmembrane regions rich in non-polar amino acids, various propensity scales have been developed [13–17]. The first protein topology predictions were largely based on the average hydrophobicity of TM segments. More recent approaches depend on statistics. Since TM regions share common amino acids, machine learning systems were trained on datasets of integral membrane proteins. Most machine learning methods rely on hidden Markov models, neural networks, or support vector machine algorithms [18–21]. Using a novel combination of hidden Markov models and artificial neural networks, Viklund and Elofasson have developed a method (OCTOPUS) that predicts the correct

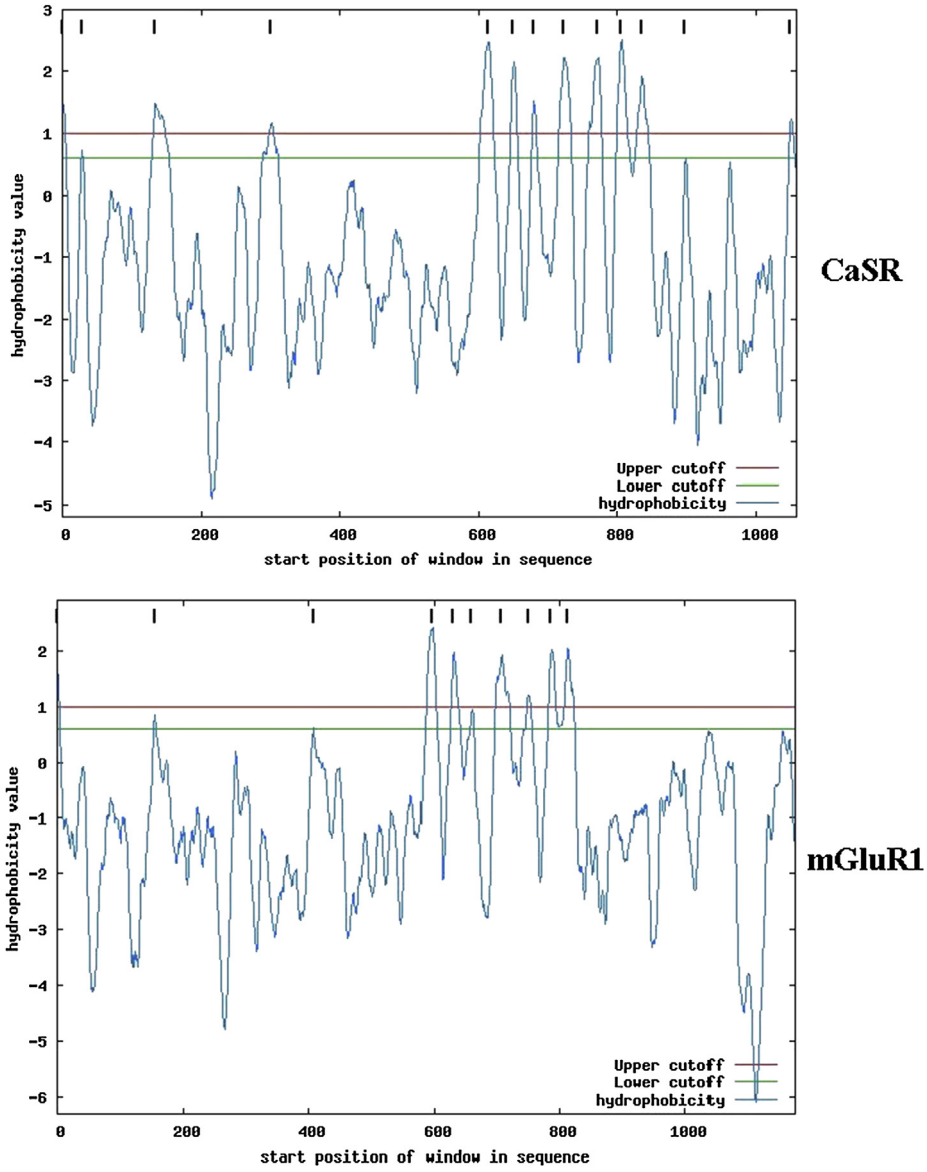

Fig. 1. A comparison of the hydrophobicity values of the calcium sensing receptor (CaSR, *Homo sapiens* #P41189, top) and the glutamate receptor (mGluR1, *Homo sapiens*, Q13255, bottom) using Mobyle 1.5 (available at mobile@pasteur). The blue lines represent plots of the hydrophobicity values with the red line indicating the upper cutoff and the green line the lower cutoff for TM helix prediction. The amino acid sequences are those published in the Swiss Protein Knowledgebase (www.uniprot.org). (For interpretation of the references to colour in this figure legend, the reader is referred to the web version of this article.)

topology for 94% of 124 sequences with known structures [22]. SPOCTOPUS predicts signal peptides [23] in addition to TM helices. The link for both is available at http://octopus.cbr.su.se/. Pore-lining regions in transmembrane protein sequences were predicted using the method (MEMSAT-SVM) of Nugent and Jones [11]: (http://bioinfo.cs.ucl.ac.uk/psipred/).

2.3. Caveolin-binding motifs

Using a GST-fusion protein-bacteriophage display library system, Couvet et al. [24] identified at least two related but distinct caveolin binding motifs, ΦxxxxΦxxΦ and ΦxΦxxxxΦ (where Φ represents an aromatic amino acid, W, Y, or F). The motifs have been shown to interact with caveolin in most proteins.

2.4. The CRAC and inverse CRAC (CARC) domains

CRAC is a short linear amino acid motif that mediates binding to cholesterol and stands for **C**holesterol **R**ecognition/Interaction **A**mino acid **C**onsensus sequence [25]. In a C- to N-terminus direction the motif consists of a branched apolar Leu (L) or Val (V) residue, followed by a segment containing 1-5 of any residues, followed by a mandatory aromatic Tyr (Y) residue, a segment containing 1-5 of any residues, and finally a basic Lys or Arg. In the one letter amino acid code the algorithm is (L/V) − X_{1-5} − (Y) − X_{1-5}- (K/R). A second cholesterol recognition domain similar to the CRAC domain (CARC) has been identified [26]. The CARC domain is comparable to the CRAC domain but exhibits the opposite orientation along the polypeptide chain ("inverted CRAC"), i.e. (K/R) − X_{1-5} − (Y/F) − X_{1-5} − (L/V). CARC is distinct from CRAC in that the central amino acid can be either Y or F.

3. Results

3.1. Comparison of the hydrophobicity profile and transmembrane (TM) helix topology in the calcium sensing receptor (CaSR) and the metabotropic glutamate receptor 1 (mGluR1)

The transmembrane (TM) helix, as described by Hilldebrand et al. [27], is a membrane-spanning 17.3 ± 3.1 (SD, N = 160) amino acid sequence with a hydrogen-bonded helical configuration, including α-, 3_{10}- and π-helices. The α-helix is very common, while the 3_{10} helix is found at the ends of the TM π-helix. Π-helices are rare. Fig. 1 compares the hydrophobicity plots of *H. sapiens* CaSR (upper) and mGluR1 (lower). Comparison of the hydrophobicity profiles of the two proteins indicates 2 additional TM helices above the upper cutoff (red line) present in the N-terminal region of CaSR whereas mGluR1 indicates 1 additional TM helix at the lower cutoff (green line); but no additional helices above the red line. CaSR and mGluR1 exhibit common heptahelical TM bundles in the C-terminal region. Use of LALIGN (see Methods) indicated minimal amino acid sequences in common within CaSR and mGluR1. Overall, CaSR (1077 aa) and mGluR1 (1194 aa) had a 28.3% identity in a 951 amino acid overlap (26-956:39-938); score: 1115 e (100000), indicating limited sequence homology. The hydrophobicity plots also indicate that both CaSR and mGluR1 contain TM helices in addition to those associated with the heptahelical bundles.

Fig. 2 illustrates the TM helix topology as predicted for CaSR (top) and mGluR1 (bottom), using the program SPOCTOPUS: a novel combination of hidden Markov models and artificial neural networks [22,23]. The topology output (top diagram in Fig. 2) represents the most likely topology as predicted by SPOCTOPUS. As shown, we find that SPOCTOPUS predicts that CaSR contains two TM helices the 200–300 residue region as well as a seven TM helical array in the 600–900 residue regions (top). In contrast, mGluR1 contains only one additional TM helix in the 400 residue region (bottom). The two diagrams labeled "Network value" indicates the estimated preference for each residue to be located among the different structural regions. The top Network Output shows the preference of being in: 1) the hydrophobic part of the membrane, 0-13Å from the membrane center, 2) the membrane water-interface, 11-18Å from the membrane center, 3) a closed-loop region, 13-23Å from the membrane center, and 4) a globular region, further than 23Å from the membrane. The bottom Network value shows the estimated preference of a particular residue to be located either on the inside or on the outside of the membrane. The prediction of TM helices in both CaSR and mGluR1 by SPOCTOPUS is consistent with the hydrophobicity profiles in Fig. 1. As also shown, both CaSR and mGluR1 contain N-terminal signal peptides (5 - 30

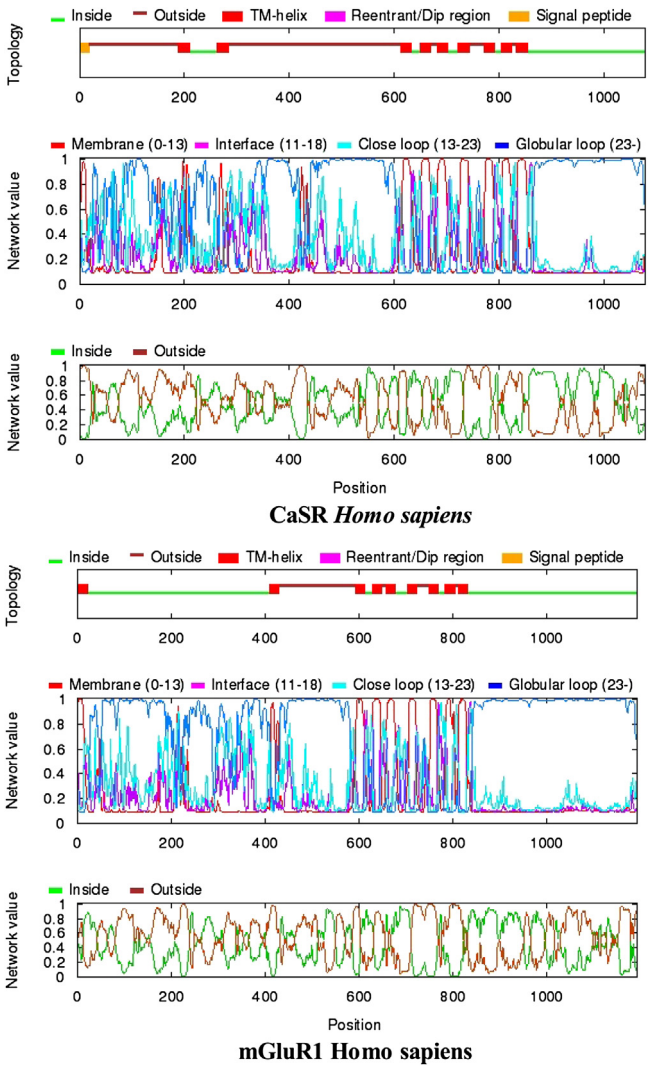

Fig. 2. Comparison of the TM helix topology as predicted for CaSR (top) and mGluR1 (bottom), using the program SPOCTOPUS: a combination of hidden Markov models and artificial neural networks [23]. The topology output (top diagrams) represents the most likely topology as predicted by SPOCTOPUS. The two diagrams labeled "Network value" indicates the estimated preference for each residue to be located in different structural regions. The top Network Value Output shows the preference of being in: 1) the hydrophobic part of the membrane, 0-13Å from the membrane center, 2) the membrane water-interface, 11-18Å from the membrane center, 3) a closed-loop region, 13-23Å from the membrane center, and 4) a globular region, further than 23Å from the membrane. The bottom Network value shows the estimated preference of a particular residue to be located either on the inside (i) or on the outside (○) of the membrane.

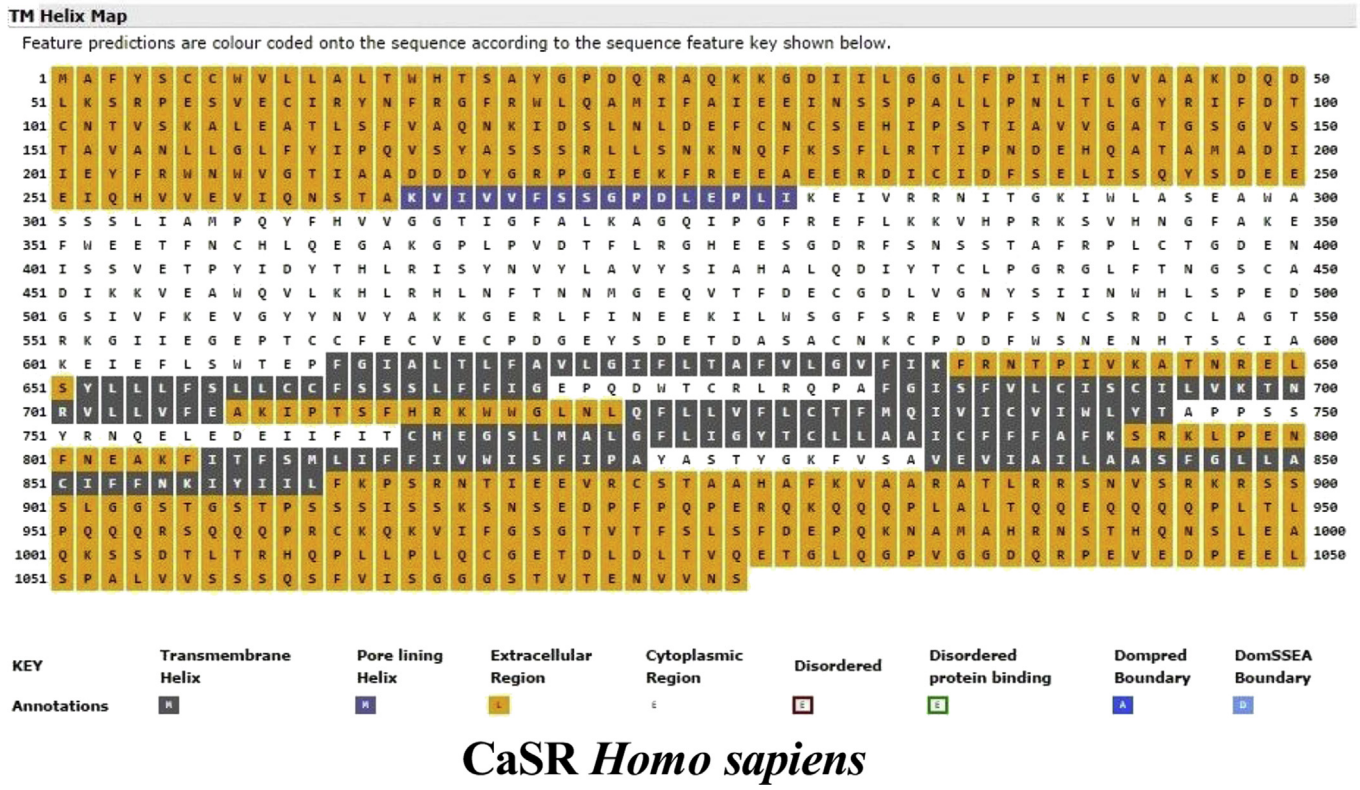

Fig. 3. The pore-lining regions and helix topology for CaSR predicted by the program of Nugent and Jones [11]) using the support vector machine-based TM topology predictor MEMSAT-SVM (see Methods). The Nugent and Jones method identifying pore-lining regions predicts: 1) the likelihood of transmembrane helices being involved in pore (channel) formation and 2) determines the number of subunits required to form a complete pore or channel. Blue squares indicate the predicted pore-lining region whereas the black squares indicate classical TM helices. (For interpretation of the references to colour in this figure legend, the reader is referred to the web version of this article.)

amino acid short sequences present at the N-terminus of a majority of newly synthesized proteins that are destined towards the secretory pathway).

Nugent and Jones have developed a method to predict pore-lining helices in transmembrane proteins [11]. By using the PoreWalker program [28] to identify pore-lining residues in transmembrane protein structures, they were able to identify pore-lining regions and predict both the likelihood of transmembrane helices being involved in pore (channel) formation and determine the number of subunits required to form a complete pore or channel (see Methods). The pore often runs parallel to TM helices, forming a path along which ions or molecules travel, with adjacent structural features determining pore specificity. As shown in Fig. 3, we find that CaSR contains a pore-lining region (^{265}K – I^{280}). This pore-lining region corresponds to the second TM helix (^{262}S–E^{282}) predicted by SPOCTOPUS (Fig. 2). In contrast, mGluR1 lacks a comparable pore-lining sequence (not shown). This is consistent with the hydrophobicity profiles in Fig. 1.

3.2. Caveolin and cholesterol binding domains of H. sapiens CaSR

The shortest sequence of amino acids in proteins that contains functional and structural information is often defined as a “motif”, whereas a conserved part of a given protein that can evolve, function and exist independently is termed a “domain”. Fig. 4 compares the distribution of the caveolin-binding motifs (highlighted in red), and CRAC/CARC (cholesterol binding) domains (highlighted in orange) within the 1078 amino acid sequence of *H. sapiens* CaSR. A cysteine-rich domain (^{537}V – C^{598}; reviewed in Ref. [9]) is highlighted largely in green and denoted by a wavy underline. The additional TM helices predicted by SPOCTOPUS (Fig. 2) are underlined with a single black line whereas members of the “classical” 7 TM G-protein helical bundles are double underlined. A 14 amino acid “linker” sequence between the cysteine-rich domain and TM-3 (^{599}I – F^{612}) reportedly supports signal transmission from the putative VFT domain to the heptahelical bundle [9]. SPOCTOPUS predicts (Fig. 2) that the N-terminal region is extracellular and highlighted in blue, whereas the C-terminal region is intracellular and highlighted in black.

As indicated in Fig. 4, SPOCTOPUS predicts that the N-terminal extracellular sequence contains 189 residues. Since a large N-terminal region composed of 400–500 residues is required [9] for bilobed Venus flytrap (VFT) domains, it is unlikely that the N-terminal region (Fig. 4) would form a VFT structure. Three caveolin binding motifs (red highlights) were identified within CaSR (Fig. 4), one in the N-terminal extracellular region and two overlapping TM-3 and TM-8 within the heptahelical bundle. Five CRAC and/or inverse CRAC (CARC) cholesterol binding motifs (orange highlights) are present; one associated with the amino-terminal region and two within the extracellular loop containing the cysteine-rich sequence. A fourth CRAC/CARC motif overlaps TM-5 of the heptahelical bundle and a fifth is within the C-terminal tail.

A comparison of CaSR and mGluR1 indicate a number of differences in helix topology, motifs and domain interfacing with the intra- and extracellular environment. Although CaSR and mGluR1 each contained 3 caveolin binding motifs, CaSR contained only 5 CRAC/CARC domains whereas mGluR1 contained 15. A CRAC/CARC domain overlap occurred with 4 of the 8 TM helices (TM-1, TM-3, TM-4, and TM-8) for mGluR1, whereas an overlap occurred for only one TM helix (TM-5) in the case of CaSR.

4. Discussion

Using the SPOCTOPUS method [23] to predict TM helices and the Nugent and Jones method [11] to identify pore-lining regions, we find that *H. sapiens* calcium sensing receptor (CaSR) contains two additional transmembrane (TM) helices as well as a pore-lining region, all within the putative Ca^{2+} sensing amino-terminal region. The two TM helices and pore-lining region are in addition to the highly conserved seven TM helix bundle within the second CaSR domain, common to all G-proteins (reviewed in Ref. [3]). Based on computational analysis, CaSR contains an initial N-terminal extracellular region containing 189 amino acids, followed by a 329 residue extracellular Ca^{2+} sensing loop. This extracellular loop contains both the cysteine-rich domain ($^{537}V-C^{598}$) (reviewed in Ref. [4]) and a 14 residue sequence ($^{599}I-F^{612}$) thought to support signal transmission [9].

One Class C G-protein-coupled receptor (metabotropic glutamate receptor mGluR1) has been characterized using x-ray crystallography (1ewt; RCSB PDB) [7] and used as a model for the VFT structure of CaSR (reviewed in Refs. [7,29]). The presence of additional TM helices within the Ca^{2+}-sensing domain (Fig. 2) would appear to rule out a Venus Flytrap-like structure in the CaSR molecule. Similar analyses of the 8 metabotropic glutamate receptors (mGluRs) indicate that most contain at least 1 additional TM helix in the same region. Although analysis of crystallographic data for the mGluR1 dimer indicates a possible bi-lobed Venus flytrap domain, extrapolation from one highly purified protein to another with a differing topology and sequence may be misleading. The finding that the Ca^{2+}-sensing receptor forms a complex with, and is upregulated by caveolin-1 [30], in human osteosarcoma cells indicates that purified crystalline CaSR may not be the physiological form of the Ca^{2+}-sensing receptor. Two of the 3 caveolin binding sites within each CaSR monomer overlap TM-3 and TM-8 within the heptahelical bundle (Fig. 4) thought to support signal transmission [9] and may identify a portion of the signaling pathway.

MAFYSCCWVLLALTWHTSAYGPDQRAQKKGDIILGGLF
PIHFGVAAKDQDLKSRPESVECIRYNFRGFRWLQAMIFAI
EEINSSPALLPNLTLGYRIFDTCNTVSKALEATLSFVAQNK
IDSLNLDEFCNCSEHIPSTIAVVGATGSGVSTAVANLLGLF
YIPQVSYASSSRLLSNKNQFKSFLRTIPNDEHQATAMADII
EYFRWNWVGTIAADDDYGRPGIEKFREEAEERDICIDFSE
LISQYSDEEEIQHVVEVIQNSTAKVIVVFSSGPDLEPLIKEI
VRRNITGKIWLASEAWASSSLIAMPQYFHVVGGTIGFALK
AGQIPGFREFLKKVHPRKSVHNGFAKEFWEETFNCHLQE
GAKGPLPVDTFLRGHEESGDRFSNSSTAFRPLCTGDENIS
SVETPYIDYTHLRISYNVYLAVYSIAHALQDIYTCLPGRGL
FTNGSCADIKKVEAWQVLKHLRHLNFTNNMGEQVTFDE
CGDLVGNYSIINWHLSPEDGSIVFKEVGYYNVYAKKGER
LFINEEKILWSGFSREVPFSNCSRDCLAGTRKGIIEGEPTC
CFECVECPDGEYSDETDASACNKCPDDFWSNENHTSCIA
KEIEFLSWTEPFGIALTLFAVLGIFLTAFVLGVFIKFRNTPI
VKATNRELSYLLLFSLLCCFSSSLFFIGEPQDWTCRLRQP
AFGISFVLCISCILVKTNRVLLVFEAKIPTSFHRKWWGLL
QFLLVFLCTFMQIVICVIWLYTAPPSSYRNQELEDEIIFITC
HEGSLMALGFLIGYTCLLAAICFFFAFKSRKLPENFNEAK
FITFSMLIFFIVWISFIPAYASTYGKFVSAVEVIAILAASFGL
LACIFFNKIYIILFKPSRNTIEEVRCSTAAHAFKVAARATL
RRSNVSRKRSSSLGGSTGSTPSSSISSKSNSEDPFPQPERQK
QQQPLALTQQEQQQQPLTLPQQQRSQQQPRCKQKVIFG
SGTVTFSLSFDEPQKNAMAHRNSTHQNSLEAQKSSDTLT
RHQPLLPLQCGETDLDLTVQETGLQGPVGGDQRPEVED
PEELSPALVVSSSQSFVISGGGSTVTENVVNS

CaSR *Homo sapiens*

Fig. 4. Analysis of the ***Homo sapiens*** CaSR amino acid sequence for transmembrane helices, pore-lining regions, protein motifs and/or domains. Extracellular amino acids are in blue; intracellular (cytoplasmic) amino acids are in black. TM helices predicted by SPOCTOPUS [23] are underlined in solid black. The classical helices in the heptahelical bundle are double underlined. Caveolin binding motifs are indicated in red; CRAC/CARC domains are highlighted in orange. A cysteine-rich domain ($^{537}V-C^{598}$) is highlighted in green and denoted by a curvy underline. (For interpretation of the references to colour in this figure legend, the reader is referred to the web version of this article.)

The extracellular Ca^{2+}-sensing receptor (CaSR) is activated allostearically by L-amino acids [29] which act, at least in part, by increasing the frequency of $[Ca^{2+}]_o$-activated oscillations in the cytoplasmic ionized Ca^{2+} concentrations. Evidence for functional significance of the amino (N)-terminal domain comes from double mutation experiments by Mun et al. [31]. These investigators identified mutations of the putative Ca^{2+}-sensing receptor Venus flytrap domain that specifically impaired only amino acid sensing, leaving Ca^{2+}-sensing intact. Conservative double mutations included residues Ser-147, Ser-170, Tyr-218, and Glu-297, with site-directed mutagenesis of Thr-145. When the mutations are compared with their positions in the CaSR sequence map (Fig. 4), only three of the five mutations (Thr-145, Ser-147, and Ser-170) were found to occur within the N-terminal extracellular domain. Tyr-218 is within an intracellular loop and Glu-297 is within the extracellular loop which also contains the cysteine-rich region. Mun et al. [31] also found that double mutants exhibited normal or near-normal sensitivity to extracellular Ca^{2+} but were resistant to increasing levels of L-phenylalanine. These findings suggest that the Ca^{2+} and L-amino acid binding sites lie within the N-terminal domain of CaSR, but are independent.

The presence of multiple caveolin- and cholesterol-binding (CRAC/CARC) motifs indicates that CaSR is concentrated within the cholesterol-rich surface caveolae of membrane lipid rafts [32,33]. This is consistent with other evidence for segregation of heterotrimeric G-proteins in cell surface microdomains (e.g. Refs. [32,33]). A CRAC motif has been previously identified in caveolin 1 (^{94}VTKYWFRY^{101}) (reviewed in Ref. [34]). Subsequent studies indicated [34] the presence of three additional inverse CRAC motifs (^{66}KIDFEDV^{71}; ^{86}KASFTTFTV^{94}; ^{96}KYWFYRLL^{103}) in CAV-1 (Q03135). Similar analyses identified 4 CRAC/inverse CRAC (CARC) motifs in CAV-2 (P51686) and 3 CRAC/CARC motifs in CAV-3 (P56539). This indicates that caveolins associated with 3 CB motifs in CaSR (highlighted in red in Fig. 4) could, in turn, bind additional cholesterol molecules and contribute a cluster of bound cholesterol molecules to the Ca^{2+}-sensing region of CaSR. As shown previously, each caveolin contains a pore-lining region [34]. Our findings suggest: 1) the cholesterol-binding domains localize the CaSR dimers to lipid rafts, 2) the N-terminal Ca^{2+}-sensing sequence of CaSR extends into intracaveolar space (not forming a VFT), and 3) pore-lining regions of CaSR dimers and bound caveolins combine to form ion channels that may play a role in monitoring ionized Ca^{2+} levels and function in cell signaling.

Conflict of interest

The authors (Dr. Gene A. Morrill, Dr. Adele B. Kostellow, Dr. Raj K. Gupta) declare no conflict of interest.

Acknowledgments

This research was supported in part by National Institutes of Health Research Grants GM-57421, HD-10463 and GM-071324.

References

[1] M. Bai, Structure and function of the extracellular calcium-sensing receptor (Review), Int. J. Mol. Med. 4 (1999) 115–125.
[2] A.M. Hofer, E.M. Brown, Extracellular calcium sensing and signaling, Natl. Rev. Mol. Cell. Biol. 4 (2003) 530–538.
[3] C. Silve, C. Petrel, C. Leroy, H. Bruel, E. Mallet, D. Rognan, M. Ruat, Delineating a Ca2+ binding pocket within the Venus flytrap module of the human calcium-sensing receptor, J. Biol. Chem. 280 (2005) 37917–37923.
[4] J. Hu, A.M. Spiegel, Structure and function of the calcium-sensing receptor: insights from natural and engineered mutations and allosteric modulators, J. Cell. Mol. Med. 11 (2007) 908–922.
[5] D. Riccardi, E.M. Brown, Physiology and pathophysiology of the calcium-sensing receptor in the kidney, Am. J. Physiol. Ren. Physiol. 298 (2009) F485–F499.
[6] M. Bai, Structure-function relationship of the extracellular calcium-sensing receptor, Cell Calcium 35 (2004) 197–207.
[7] N. Kunishima, Y. Shimada, Y. Tsuji, T. Sato, M. Yamamoto, T. Kumasaka, S. Nakanishi, H. Jingami, K. Morikawa, Structural basis of glutamate recognition by a dimeric metabotropic glutamate receptor, Nature 407 (2000) 971–977.
[8] J. Hu, A.M. Spiegel, Naturally occurring mutations of the extracellular Ca2+-sensing receptor: implications for its structure and function, Trends Endocrinol. Metab. 14 (2003) 282–288.
[9] M.A. Khan, A.D. Conigrave, Mechanisms of multimodal sensing by extracellular Ca2+-sensing receptors: a domain-based survey of requirements for binding and signaling, Br. J. Pharmacol. 159 (2010) 1039–1050.
[10] E.M. Epand, B.G. Sayer, R.F. Epand, Caveolin scaffolding region and cholesterol-rich domain in membranes, J. Mol. Biol. 345 (2005) 339–350.
[11] T. Nugent, D.T. Jones, Detecting pore-lining regions in transmembrane protein sequences, BMC Bioinfomatics 13 (2012) 169–178.
[12] M. Goujon, H. McWilliam, W. Li, F. Valentin, S. Squizzato, J. Paern, R. Lopez, A new bioinformatics analysis tools framework at EMBL-EBI, Nucleic Acids Res. 38 (2010) W695–W699.
[13] J. Kyte, R.F. Doolittle, A simple method for displaying the hydrophobic character of a protein, J. Mol. Biol. 157 (1982) 105–132.
[14] D. Eisenberg, W. Wilcox, A.D. McLachlan, Hydrophobicity and amphiphilicity in protein structure, J. Cell. Biochem. 31 (1986) 11–17.
[15] D.M. Engelman, T.A. Steitz, A. Goldman, Identifying nonpolar translayer helices in amino acid sequences of membrane proteins, Annu. Rev. Biophys. Biophys. Chem. 15 (1986) 321–353.
[16] W.C. Wimley, S.H. White, Experimentally determined hydrophobicity scale for proteins at membrane interfaces, Nat. Struct. Biol. 3 (1996) 842–848.
[17] G. Zhao, E. London, Strong correlation between statistical transmembrane tendency and experimental hydrophobicity scales for identification of transmembrane helices, J. Membr. Biol. 229 (2009) 165–168.
[18] J.L. Popot, C. Vitry, On the microassembly of integral membrane proteins, Annu. Rev. Biophys. Biophys. Chem. 19 (1990) 369–403.
[19] B. Rost, P. Fariselli, R. Casadio, Topology prediction for helical transmembrane proteins at 86% accuracy, Protein Sci. 5 (1996) 1704–1718.
[20] E.L. Sonnhammer, G. von Heijne, A. Krogh, A hidden Markov model for predicting transmembrane helices in protein sequences, Proc. Int. Conf. Intel. Sys. Mol. Biol. 6 (1998) 175–182.
[21] C. Yuan, R.U. O'Connell, P.I. Feinberg-Zadek, I.J. Johnson, S.N. Treistman, Bylayer thickness modulates the conductance of the BK channel in model membranes, Biophys. J. 86 (2004) 3620–3633.
[22] H. Viklund, A. Elofsson, OCTOPUS: improving topology by two-track ANN-based preference scores and an extended topological programmer, Bioinfomatics 24 (2008) 1662–1668.
[23] H. Viklund, A. Bernsel, M. Skwark, A. Elofsson, SPOCTOPUS: a combined predictor of signal peptides and membrane protein topology, Bioinfomatics 24 (2008) 2928–2929.
[24] J. Couvet, M. Sargiacomo, M.P. Lisanti, Interaction of a receptor tyrosine kinase, EGF-R, with caveolins, J. Biol. Chem. 272 (1997) 30429–30438.
[25] H. Li, V. Papadopoulos, Peripheral-type benzodiazepine receptor function in cholesterol transport. Identification of a putative cholesterol recognition/interaction amino acid sequence and consensus pattern, Endocrinology 139 (1998) 4991–4997.
[26] C.J. Baier, J. Fantini, F.J. Barrantes, Disclosure of cholesterol recognition motifs and transmembrane domains of human nicoticin acetylcholine receptor, Sci. Reports 1:69, http://dx.doi.org/10.1038/srep00069.
[27] F.W. Hilldebrand, S. Lorenzen, A. Goede, R. Preisser, Analysis and prediction of helix-helix interactions in membrane channels and transporters, Proteins 64 (2006) 253–262.
[28] M. Pellegrini-Calace, T. Malwald, J.M. Thorton, A novel tool for the identification and characterization of channels in transmembrane proteins from their three-dimensional structure, PLOS Comput. Biol. 5 (2009) 1–16.
[29] A.D. Conigrave, S.J. Quinn, E.M. Brown, Cooperative multi-modal sensing and therapeutic implications of the extracellular Ca(2+) sensing receptor, Trends Pharmacol. Sci. 10 (2000) 401–407.
[30] S.Y. Jung, J.O. Kwak, H.W. Kim, D.S. Kim, S.D. Ryu, C.B. Ko, S.H. Cha, Calcium sensing receptor forms complex with and is up-regulated by caveolin-1 in cultured human osteosarcoma (Saos-2) cells, Exp. Mol. Med. 30 (2005) 91–100.
[31] H.-C. Mun, E.L. Culverston, A.H. Franks, C.A. Collyer, R.J. Clifton-Bligh, A.D. Conigrave, A double mutation in the extracellular Ca2+-sensing receptor's Venus flytrap domain that selectively disables L-amino acid sensing, J. Biol. Chem. 280 (2005) 29067–29072.
[32] P. Oh, J.E. Schnitzer, Segregation of heterodimeric G proteins in cell surface microdomains, G(q) binds caveolin to concentrate in caveolae, whereas G(i) and G(s) target lipid rafts by default, Mol. Biol. Cell. 12 (2001) 685–698.
[33] H.H. Patel, F. Murray, P.A. Insel, G-Protein-coupled receptor signaling components in membrane raft and caveolae microdomains, Handb. Exp. Pharmacol. 186 (2008) 167–184.
[34] G.A. Morrill, A.B. Kostellow, R.K. Gupta, The pore-lining regions in cytochrome c oxidases: a computational analysis of caveolin, cholesterol and transmembrane helix contributions to proton movement, Biochim. Biophys. Acta 1838 (2014) 2838–2851.